Mesoporous GO-TiO₂ nanocomposites for flexible solid-state supercapacitor applications

To cite this article before publication: Priyanka Rani *et al* 2020 *Mater. Res. Express* in press https://doi.org/10.1088/2053-1591/ab66f6

Mesoporous GO-TiO_2 Nanocomposites for Flexible Solid-state Supercapacitor Applications.

Priyanka Rani,[1] Arup Ghorai,[1] Saptarsi Roy,[2] Dipak K Goswami,[3] Anupam Midya,[1] Samit K Ray[4]*

[1]*School of Nanoscience and Technology, Indian Institute of Technology Kharagpur, Kharagpur 721302, India,*

[2]*Department of Mechanical Engineering, Aryan Institute of Engineering and Technology, Bhubaneswar, 752050, India*

[3]*Department of Physics, Indian Institute of Technology Kharagpur, Kharagpur 721302, India*

[4]*S. N. Bose National Centre for Basic Sciences, Kolkata 700 106, India*

Corresponding email: anupam.midya@iitkgp.ac.in; anumidya@gmail.com:

Abstract:

Fabrication of flexible solid-state supercapacitor is a field of paramount importance because of its potential application in portable devices. In this article, graphene oxide and titanium dioxide hybrid (GO-TiO_2) nanocomposites of different compositions are employed for the fabrication of flexible solid-state supercapacitors. An easy, fast, scalable and controlled sol-gel method is devised for GO-TiO_2 nanocomposites growth from different amounts of graphene oxide and titanium isopropoxide at atmospheric pressure. Highly monodispersed rutile TiO_2 nanospindle is homogenously grafted on GO by a controlled HCl catalyzed reaction. BET N_2 adsorption desorption isotherm analysis confirms formation of the mesoporous structure having a large specific surface area favourable for faster reversible adsorption and desorption of ions. An optimum composition of GO-TiO_2 nanocomposite (TG25) exhibits a high areal specific capacitance of 73.43 mF/cm^2 at a current density of 0.5 mA /cm^2 due to formation of electrical double layer in a solid-state supercapacitor. The fabricated device shows high power density (3.5 mW/ cm^2), a high energy density (0.007 mWh/ cm^2), good flexibility and excellent cycling stability, 92% specific capacitance retention after 10,000 continuous charge-discharge cycles. Finally, three supercapacitors in a series have illuminated a red LED, indicating the nanocomposite as a potential candidate for energy storage technology.

Keywords: Rutile TiO_2, GO, Nanospindles, Nanocomposites, gel electrolyte, Supercapacitors.

Introduction:

Solid-state supercapacitors having a high power density and high specific capacitance have attracted great attention for their high stability, flexibility, long term use and they are complementary of battery in energy storage applications.[1] The performance of electrical double layer (EDL) supercapacitors, store energy due to reversible charge accumulation and desorption, can be improved by engineering the critical parameters such as increasing the electrical conductivity, [2] surface area and interconnectivity of active electrode materials.[3] In this respect, various transition metal oxides such as MnO_2, Nb_2O_5, RuO_2, Co_3O_4, and $Ni(OH)_2$ have been employed in supercapacitor having different structure and morphology which attributed to high specific surface area. In addition, transition metal oxides shows large pseudocapacitance due to surface redox reactions.[4] RuO_2 is one of the most promising electrode materials due to its ultrahigh pseudocapacitance (700 F g^{-1}), low resistivity, high chemical and thermodynamic stability under electrochemical environments. However it's application is restricted due to the high cost.[5] Co_3O_4 has high theoretical capacitance (up to 3560 F g^{-1}), and well-defined redox behavior but delivers poor rate capability and reversibility due to its poor electrical conductivity and large crystallite size.[6] MnO_2 can also be used as electrode material because it is predicted to show a high capacitance and it is inexpensive. But its poor conductivity (10^{-5}–10^{-6} S cm^{-1}) limits the charge/discharge rate for high-power applications.[7] TiO_2 forms conventional electrical double-layer capacitor (EDLC) and shows rectangular cyclic voltammetry curves which make it a promising electrode material for supercapacitor devices. TiO_2 nanostructures have tunable high surface area, low cost, environmentally benign behavior and long term chemical stability which make it attractive

material in bio-implant and other sophisticated energy storage application.[8] However, it has a lower theoretical capacity (1206 F g^{-1}) and its high resistivity results in large internal resistance, slow ion diffusion and poor electron transfer.[9],[10] On the other hand, supercapacitors of the bare carbon material exhibit high surface area, good conductivity, and restricted ionic accessibility.[11] Therefore, it is interesting to pair transition metal oxides such as TiO_2 with carbonaceous materials such as graphene to form composites to extract the benefits of both materials reducing the limitation of each material.[12] Restacking of graphene sheets can be minimized by using TiO_2 nanoparticles as intercalator, which eventually increases the specific surface area, sustaining better access of ionic electrolyte. Graphene, a sp^2-hybridized two-dimensional carbon sheet, exhibits extraordinary mechanical flexibility,[13] high chemical stability, high electrical conductivity, and high specific surface area (2630 m^2 g^{-1}) attractive for the flexible device applications.[14],[15]

Few graphene-TiO_2 nanocomposites have been synthesized at high pressure or using surfactants or additives to minimize the agglomeration of TiO_2.[16],[17] For example, Xiang et al.[18] have reported shape and coupling effects of hydrothermally synthesized reduced graphene oxide-TiO_2 composites for supercapacitor applications using expensive nickel disk as the current collector. A bare TiO_2 nanotube array is also employed in supercapacitor to achieve a low aerial capacitances of 2.6 mF cm^{-2}.[19] Size-tunable anatase TiO_2 nanospindles assembled with titanium oxynitride/titanium nitride graphene nanocomposites show high cycling performance in rechargeable lithium ion batteries.[23] Flexible composite film of rGO/TiO_2, grown at high temperature (600 °C), is employed as supercapacitor electrode in three-electrode cell configuration.[20] However, controlling the size of particles, their morphology and dispersion density of inorganic nanocrystals on graphene sheets, which eventually increase the electrical

conductivity and surface area leading to a superior supercapacitor performance in two electrode configuration is still a challenge, and needs more attention.

Here, we report an easy, controlled, in-situ growth of mesoporous GO-TiO_2-nanocomposites of different compositions at atmospheric pressure. The evolutions of HCl catalyzed TiO_2 nanospindles of rutile phase on graphene platform are monitored by SEM, TEM, XPS, XRD and Raman spectroscopy techniques. The nanocomposites are employed in flexible solid-state supercapacitor device using acetylene black conducting filler and a gel PVA-H_3PO_4 electrolyte on flexible steel plate electrode. The devices show excellent cyclic stability (92% specific capacitance retention after 10,000 charge-discharge cycles), high specific capacitance and power density, indicating the GO-TiO_2 nanocomposite as a potential candidate for energy storage applications. The novelty of the work lies in the easy growth of mesoporous GO-TiO_2 nancomposite and demonstration of flexible solid-state supercapacitor igniting LED bulbs.

Materials and Characterizations:

Graphite powder, $KMnO_4$, Sodium nitrate, Titanium tetraisopropoxide, 30% H_2O_2, and conc. H_2SO_4 (98%), HCl were purchased from Sigma Aldrich and used without further purifications. Ultra pure water was obtained from Sartorius ultra pure water purification system (Model Arium Comfort II) and ultra pure water was used for the whole experiment.

Physical Characterization

The morphologies of the prepared samples were characterized by Field emission scanning electron microscopic (FESEM). FESEM Images were taken by SUPRA 40 Field Emission Scanning Electron Microscope (Carl Zeiss SMT AG, Germany). High Resolution Transmission

Electron Microscopy images were taken by JEOL 200 keV instrument. The phase analysis and structure were investigated by X-ray diffraction measurements. Raman spectroscopy (Lab RAM HR JovinYvon) is carried to study the crystalline quality and local structural disorder of nanocomposites. The surface chemical composition and chemical states of the elements in the samples were identified by X-ray photoelectron spectroscope (model PHI 5000 Versa Probe II (ULVAC, PHI Inc.). The electrochemical properties and capacitance measurements of the GO-TiO_2 nanocomposites electrodes were characterized using cyclic voltammetry (CV), galvanostatic charge discharge (GCD) and electron impedance spectroscopy (EIS) using an electrochemical station (Gamry, Model 1000 interface) with a two-electrode configuration using H_3PO_4/PVA electrolyte, GO-TiO_2 nanocomposite active material deposited on electrodes on steel plate. The EIS measurements were conducted at varying frequency from 0.001 Hz to 10 kHz with amplitude of 5 mV at an open-circuit voltage. The CV and GCD were tested between 0 and 1 V, and the areal specific capacitance (mF/cm^2) was calculated from discharge curves from the following equation.

$$C = \frac{(I\Delta t)}{(A\Delta V)}$$

Where I , Δt , A and ΔV is discharged current, discharge time, area of electroactive material and potential window, respectively.

At a given scan rate the specific energy density (E.D; mWh/cm^2) and Specific power density (P.D; mW/cm^2) of the device was calculated from the following equation

$$E.D = \frac{C\Delta V^2}{7200}$$

$$P.D=\frac{E.D\times 3600}{\Delta t}$$

Δt is the duration (sec) of the discharge half-cycle in the discharge curve.

Synthesis of GO

Graphite oxide was synthesized by the modified Hummer and Offeman's method with graphite powder.[21] Graphite powder was oxidized using $KMnO_4$ in presence of conc H_2SO_4. Graphite oxide slurry was filtered and exfoliated in DI water by ultrasonication in a bath sonicator as described in our previous work.[22] The graphene oxide was purified sequentially by centrifugation and dispersion of the precipitations in DI water. The GO was collected after removing small and big graphene oxide particle at a high and low centrifugation speed, respectively.

Synthesis of GO-TiO_2

The schematic of GO-TiO_2 nanocomposite synthesis is shown in Figure 1. Concisely, 0.937µL of titanium tetraisopropoxide (TTIP) was dissolved in 40 ml ultrapure DI containing 5 ml HCl under vigorous stirring with a magnetic stirrer for 30 min. Different amounts of as-synthesized GO (10, 25, 50 and 100 mg) are added to the solution and stirred for 30 min, separately. After that, the temperature of the growth solution was maintained at 120°C for 2 hr for each sample. A gray precipitation was obtained. The resultant precipitation was washed with distilled water for three times by centrifugation at 10,000 rpm after dispersing and followed by discarding the supernatant to remove remaining ions in the by-product. The precipitation was collected and

dried in an oven at 100 °C for 12 hr for further characterization and device fabrications. Few control TiO_2 samples were also prepared without addition of GO at similar condition using different acid concentrations (0.5 M HCl, 0.5 M HNO_3, 1M HCl). The resultant GO-TiO_2 nanocomposites were termed as TG10, TG25, TG50, and TG100 prepared using 10, 25, 50, and 100 mg of GO, respectively.

Supercapacitor device fabrication:

Electrodes comprised of GO-TiO_2 nanocomposite as active material was prepared by mixing the 85:15 mixture of GO-TiO_2 nanocomposite and acetylene black in N, N-dimethylformamide (DMF). The solution of the active material was prepared by stirring the mixture of GO-TiO_2 nanocomposites and acetylene black for overnight at 60 °C in DMF. The black color solution was drop casted on to stainless steel plates (0.01 mm width) and dried at 80 °C for 30 min in the oven. The active layer film was soaked in gel electrolyte aq. PVA-H_3PO_4 gel electrolyte for 10 min. The gel electrolyte was prepared by dissolving 1g PVA in 10 ml DI water at 60 °C for 12 hr, then 1 ml H_3PO_4 was added into the solution and stirred for 2 hr. After drying in an oven for 2 hr at 60 °C, the electrodes were kept for 24 hr at room temperature. Next, the two symmetric fabricated electrodes were sandwiched carefully. PVA plays a dual role here as a binder to hold the active layer as well as a separator between two electrodes preventing shorting. To evaporate extra amount of water, the device was further dried at 60 °C in an oven for 2 hr before the measurement was performed.

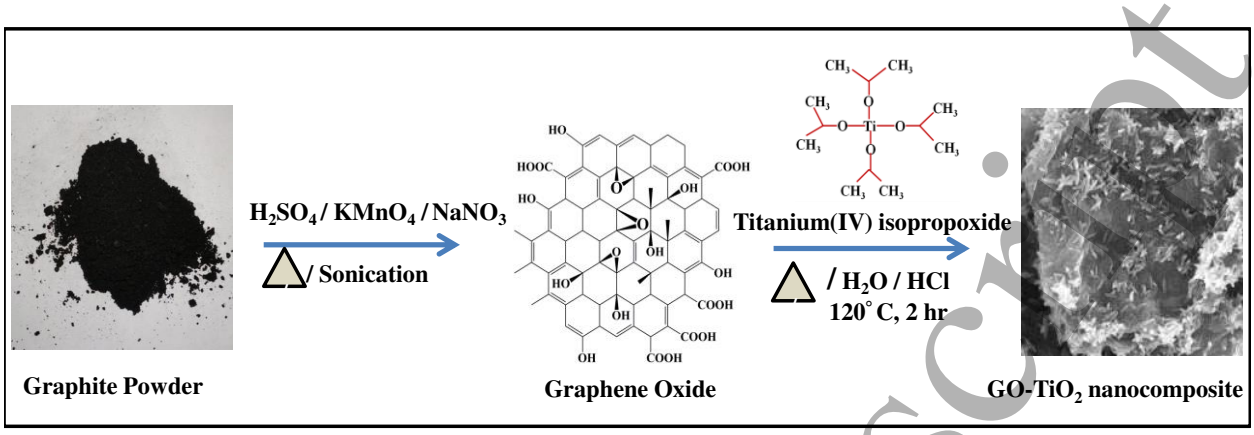

Figure 1: Schematic diagram of the evolution of TiO_2 nanospindles on graphene oxide.

Results and Discussions:

Figure 2(a) shows the FESEM image of agglomerated TiO_2 nanospindles in the absence of GO. A typical wrinkle structure of multilayer GO sheet is found in FESEM image, as shown in Figure 2(b). Whereas homogenously dispersed nanospindles on GO is shown in Figure 2(c). Incorporation of different proportions of GO precursor to the same TTIP amount (0.1:1, 1: 0.25:1, 1: 0.5:1 and 1:1) dispersion density of TiO_2 nanospindles can be tailored on GO sheets as shown in Figure S1 (ESI). Compared with homogeneous growth in the solution, the nanospindles prefer to nucleate heterogeneously at the defect sites (oxygen containing moieties) on the GO sheets so free unattached single nanospindles can't be found in the product. There is no effect seen on morphology, including the size and shape by varying the reaction time after two hours, while keeping other conditions constant. Nanospindles are grafted uniformly onto the graphene oxide sheets after induction of GO to the TTIP precursor, keeping the nanospindle-shape of TiO_2 unchanged. However, the size of TiO_2 nanospindles changes from 154 to 311 nm in length and

46 to 118 nm in diameter, as shown in Table S1 (ESI) with the varying proportion of GO from 1:0.1 to 1:1.

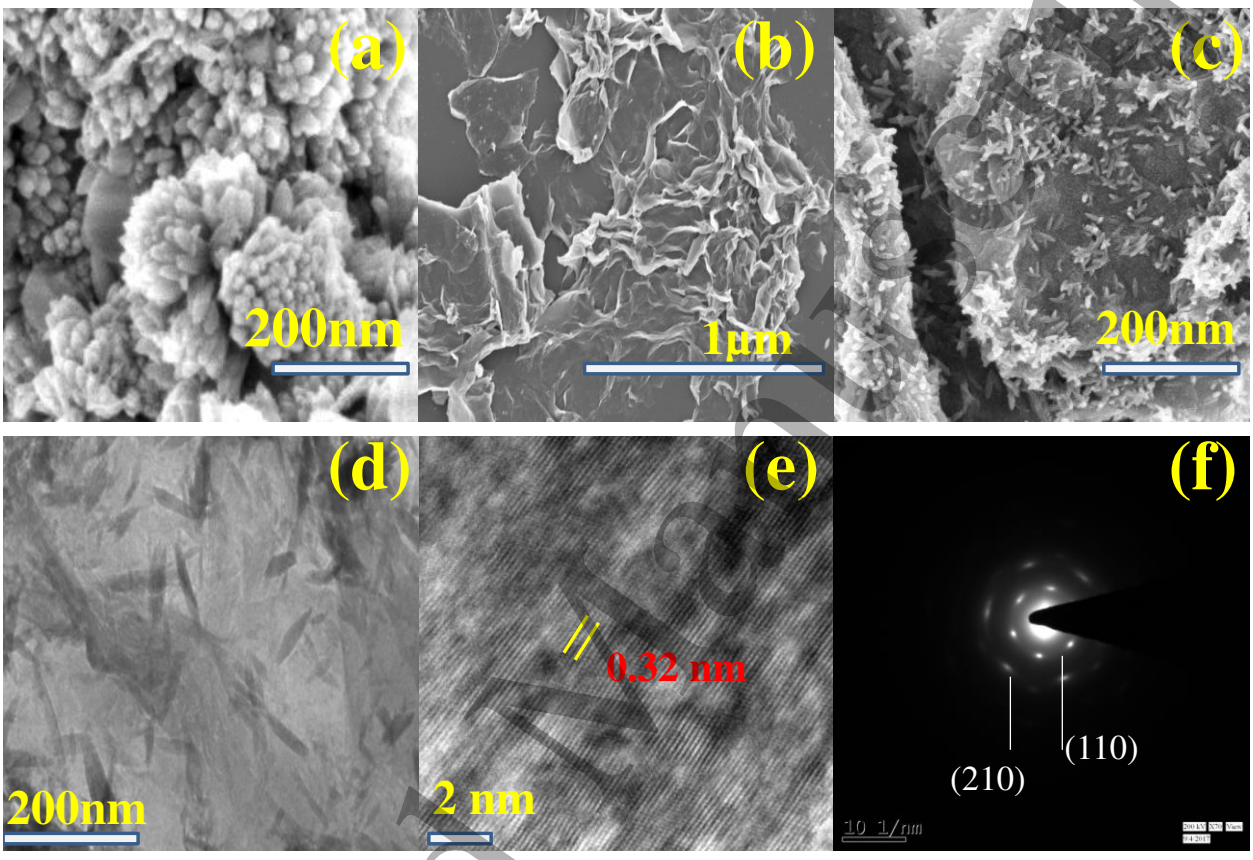

Figure 2: (a) Typical FESEM image of bare TiO_2; (b) graphene oxide; (c) TG 25. (d) Typical TEM image of TG25; (e) HRTEM image of TG25; (f) SAED pattern of TG25.

Typical FESEM image of TG25 is shown in Figure 2(c) where ~268 nm long nanospindle of ~ 78 nm diameter is homogenously grafted on GO. Figure 2 (d) shows the TEM images of TiO_2 nanospindle grafted on graphene oxide in TG25. Presence of TiO_2 prevents the restacking of graphene oxide layers and expected to exhibit a higher specific surface area which is essential for supercapacitor applications.[23] It may be noted that after a prolong sonication and washing TiO_2 nanospindles are remain attached to GO sheets, indicating a strong interaction between GO sheets and TiO_2 nanospindles. This intimate hybridization endows easy and fast charge transport

between GO and TiO_2 nanospindles beneficial for improved supercapacitor performance. The lattice fringe spacing of TiO_2 nanoparticle in HRTEM image (Figure 2 (e)) is found to be 0.32 assigned to the (110) inter planner distance of the rutile phase.[24]·[25] Selected area electron diffraction (SAED) patterns confirm good crystallinity and the lattice planes of the pure tetragonal-rutile TiO_2 phase.

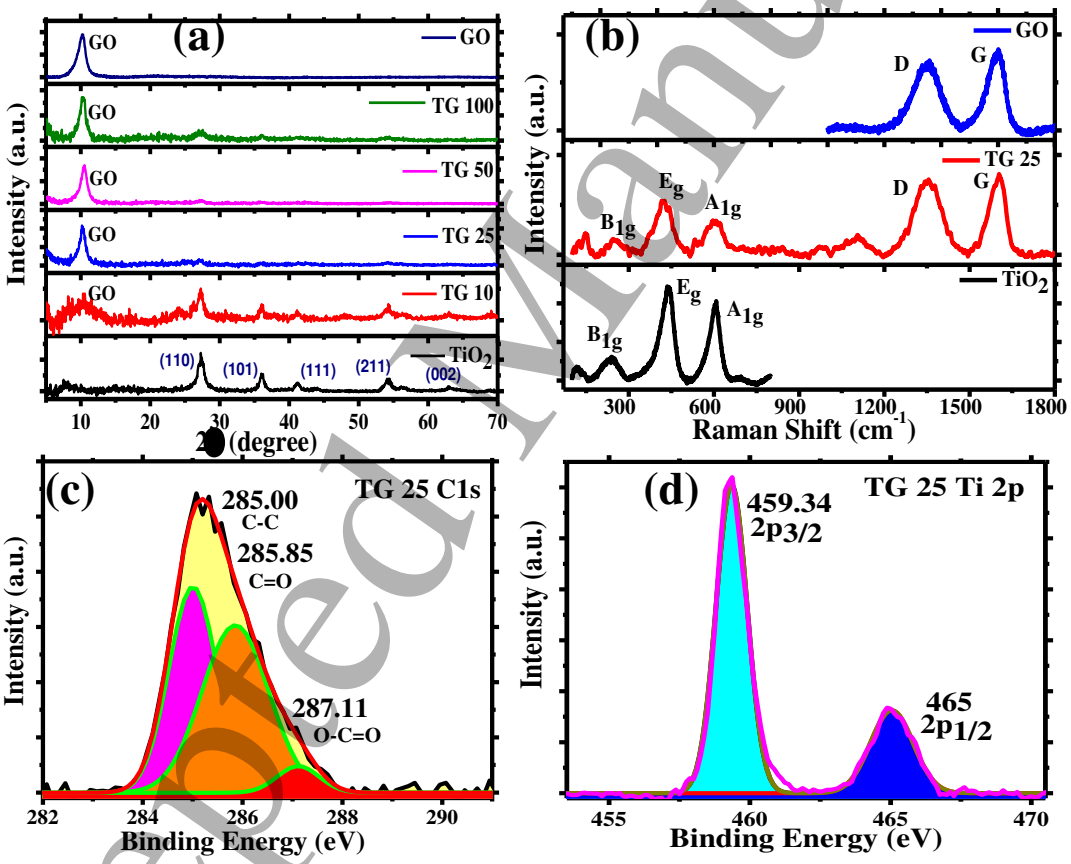

Figure 3: (a) Typical XRD patterns of bare TiO_2 and graphene oxide and TG25. (b) Raman spectra of different GO-TiO_2 nanocomposites. (c) X-ray photoelectron spectra of core level C1s electron of TG25. (d) Ti2p core level electron of TG25.

The crystal structure of TiO_2, GO-TiO_2 nanocomposites, and graphene oxide were characterized using X-Ray diffraction (XRD) analysis and the XRD patterns are shown in Figure 3(a). For TiO_2 and GO-TiO_2 nanocomposites, all of the peaks can be indexed as the tetragonal rutile phase with primitive lattice, space group- P42/mnm (136), and lattice constant a = b=4.601 c=2.956 from (JCPDS 89-0552). Interestingly, it is observed that the concentration of hydrochloric acid is critical to obtain Rutile phase TiO_2. Below 1.0 M concentration of HCl produces a mixture of rutile and anatase. Whereas above 0.5 M concentration of nitric acid produces spherical particles of anatase phase as shown in Figure S2 (ESI). When the concentration of hydrochloric acid in the solution is higher than 1.0 M, the product is nanospindle of pure rutile phase, (Figure S3, ESI). Even at the same concentration, hydrochloric acid is more effective for the formation of the rutile phase than nitric acid. [26] From above observations, we can conclude that HCl plays major role in the reaction: (i) due to an acidic medium, hydrolysis rate of TTIP got suppressed and slowed down and (ii) HCl is the major factor for the formation of the nanospindle shape of TiO_2.

The bonding structures of the GO-TiO_2 nanocomposites were characterized by Raman spectroscopy shown in Figure 3(b). The characteristic Raman peaks for TiO_2 and TG25 nanocomposites are observed at ~ 441 and 606 cm^{-1} attributed to the E_g and A_{1g} modes of rutile TiO_2, respectively. Two characteristic peaks are observed for bare GO at ~ 1349 and 1592 cm^{-1}, and for TG25 at ~ 1352 and 1597 cm^{-1}, corresponding to the well-defined D and G bands for the defect and graphitized structures, respectively. The D-band corresponds to the disorder with sp^3 structural imperfections. Therefore, the intensity ratio (I_D/I_G) for GO is found to be 0.83, signifying the presence of the large amount of defect (sp^3 C) in the sample. The change of I_D /I_G from 0.83 to 1.30 with the increasing proportion of TiO_2 indicates a strong hybridization

of TiO_2 and graphene oxide. Raman spectra of GO and different GO-TiO_2 nanocomposites are shown in Figure S4.

The nanocomposite formation is also investigated by X-ray photoelectron spectroscopy (XPS). Figure 3(c) shows the C1s electron binding energy peaks, with a binding energy of 285 eV attributed to the C–C and C=C bonds, while the peaks centered at the binding energies of 285.85, 287.11eV correspond to carbonyl (C=O) and carboxyl (O-C=O) carbon, respectively. The presence of Ti2p core level photoelectron spectrum of Ti $2p_{3/2}$ at 459.34 eV and Ti $2p_{1/2}$ at 465 eV in Figure 3(d) is a signature of Ti (IV). Figure S5 (ESI) shows the comparative photoelectron spectra of Ti2p core level electron for different compositions of nanocomposite. The broadening of the peak for Ti2p core level electron with the increase in the proportion of GO in Figure S5 (ESI) indicates intimate mixing of TiO_2 and GO.

(a)

Sample	Specific surface area (m^2/g)	Pore diameter (nm)
TG 25	96.38	12.48
TG 50	84.74	11.87
GO	38.54	32.4
TiO_2	90.51	18.3

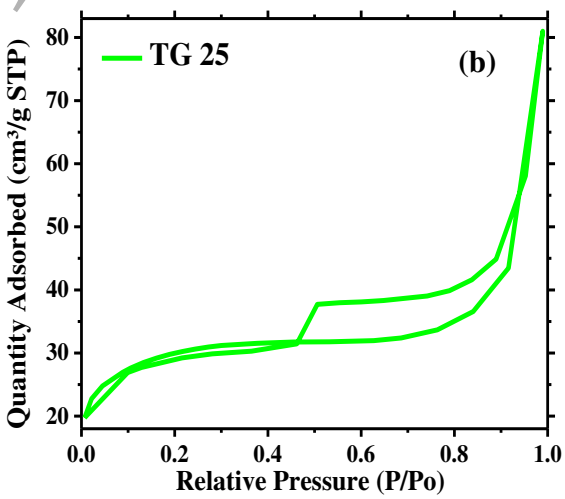

Figure 4: (a) Textural properties of GO-TiO_2 nanocomposites; (b) BET N_2 adsorption–desorption isotherm of TG25.

To get an insight into the surface property and supercapacitor performance of the nanocomposites, the specific surface area, a pore diameter of bare TiO_2, TG 25, TG50 and bare GO are investigated by BET nitrogen adsorption-desorption isotherm measurements

using Beckman Coulter SA3100 surface area analyzer. Specific surface area and pore diameter of nanocomposites are tabulated in (Figure 4a). TG 25 has shown higher surface area than TG50, bare TiO_2 and bare GO. The high specific surface area of TG25 nanocomposite may attribute to a superior specific capacitance performance in a supercapacitor. From BET measurement, the average pore diameter of TG25 is found to be 12.48 nm, indicating mesoporous nature of the electrode material which allows easy adsorption and desorption of smaller H^+ (1.2 Å) and PO_4^{3-} (2.38Å) ions and hence contributing to the capacitance of the supercapacitor. The TG25 shows type IV isotherm (Figure 4b) which is a characteristics of mesoporous structures.

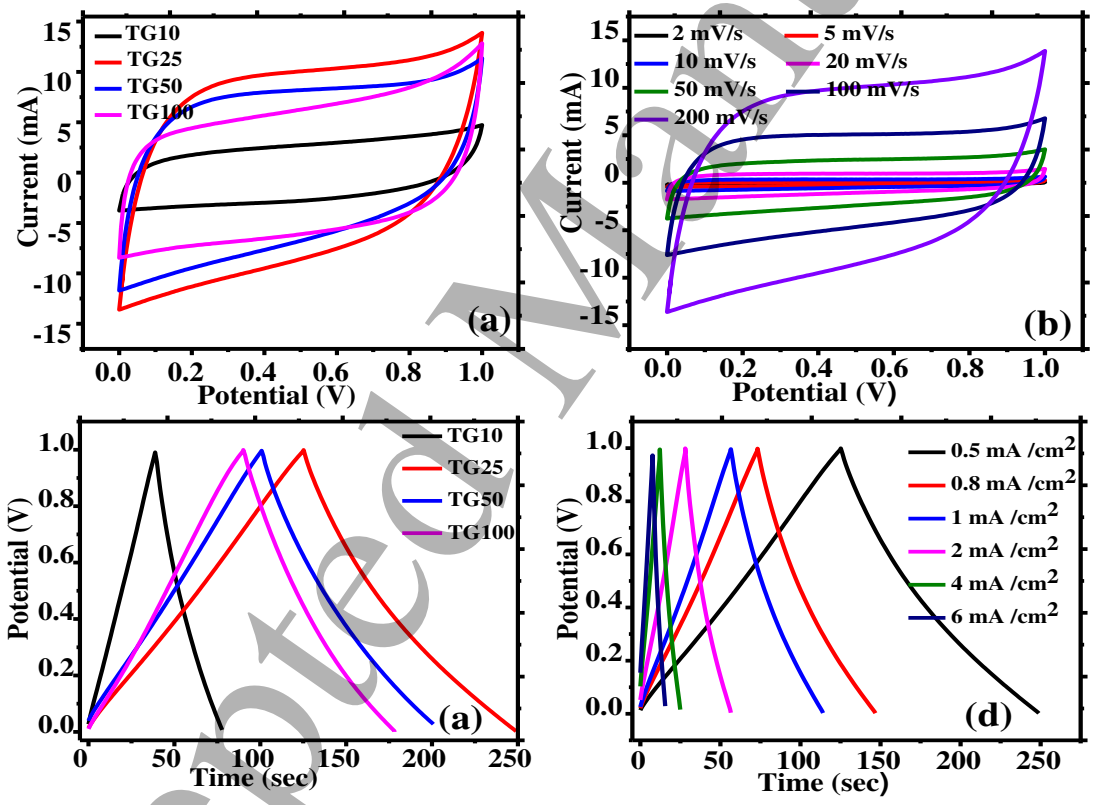

Figure 5: Typical CV curves of (a) different compositions of GO in TiO_2 at 200 mV/s scan rate; (b) TG 25 at different scan rates. Charge-discharge curves of (c) different compositions of GO-TiO_2 at 0.5 mA/cm^2 current density; (d) TG25 at different current densities.

Electrochemical charge storage properties of the fabricated solid-state supercapacitor devices were evaluated by cyclic voltammetry (CV). Figure 5(a) presents the steady state CV curves of GO-TiO_2 based solid-state supercapacitors of different compositions at a scan rate 200 mV/s. The nearly rectangular shape and enclosed area under the CV curves of all compositions indicate that the supercapacitor performance is composition dependent. The TG25 based supercapacitor shows the highest specific capacitance value because of the optimum composition of GO and TiO_2 provides good electrical contact and maximum surface area (see Table S2 ESI). Figure 5 (b) represents the CV curve of TG25 based supercapacitor at various scan rates (from 2 to 200 mV/s). The CV curves of the TG25 based supercapacitor maintain nearly rectangular shapes without having a faradic current at all the scan rates, indicating its excellent capacitive behavior originating from the electrical double layer (EDL) formation. It may be noted that the bare TiO_2 has a very low electrochemical capacitance (<40 μF cm^{-2}) because of its low conductivity and negligible faradic capacitance.[27]

Galvanostatic charge-discharge (GCD) curves are shown in Figure 5 (c) and (d) for different compositions at 0.5 mA/cm^2 current density and different current densities of TG25 based device, respectively. The charge-discharge curves are nearly triangle shape having a negligible internal resistance (IR) drop, indicating easy adsorption and desorption of ions. According to the GCD curves, the specific capacitances of the composites are calculated in the potential windows ranging from 0 to 1V. It is found that the TG25 based supercapacitor shows a highest specific capacitance of ~73.43 mF/cm^2. The specific capacitance value of the TG25 based supercapacitor is compared to that of other GO/RGO-metal oxide based solid-state supercapacitor and displayed in Table 1. The fabricated TG25 based device outperforms other devices, indicating the GO-TiO_2 as a potential candidate for energy storage applications.

Electrode Material	Method	Specific capacitance	Potential window	Cyclic stability/ Specific capacitance retention	reference
Multilayer hybrid films of graphene and titanium dioxide	Layer-by-layer (LBL) self-assembly technique	0.857 mF cm^{-2}	-0.1-0.7V	98% capacity retention after 1500 cycles.	[28]
rGO/TiO_2 NR/rGO	Hydrothermal preparation	114.5 F g^{-1}	0-0.8V	85% of its initial capacitance after 4000 cycles.	[29]
Carbon/TiO_2/reduced graphene oxide composite	Vapour-induced phase separation and self-assembly processes	23.6mF cm^{-2}	-0.2-0.8V	97.6 % maintenance of the initial capacity after 500 cycles	[2]
NF/rGO/H-Fe_2O_3	Surfactant-free hydrothermal method	37.88 mF cm^{-2}	0-1.5V	97% of capacitance retention after 10000 cycles	[30]

MnO_2-deposited graphene fibers	Facile wet-spinning assembly method	59.2 mF cm^{-2}	0-1.6 V	92.7% initial capacitance retention after 8000 cycles	[31]
GO-TiO_2	Solvothermal at atmospheric pressure.	73.43mF cm^{-2}	0-1 V	92% capacity retention after 10000 cycles	This Work

Table 1: Comparative performance of GO/RGO-metal oxide based solid-state supercapacitors

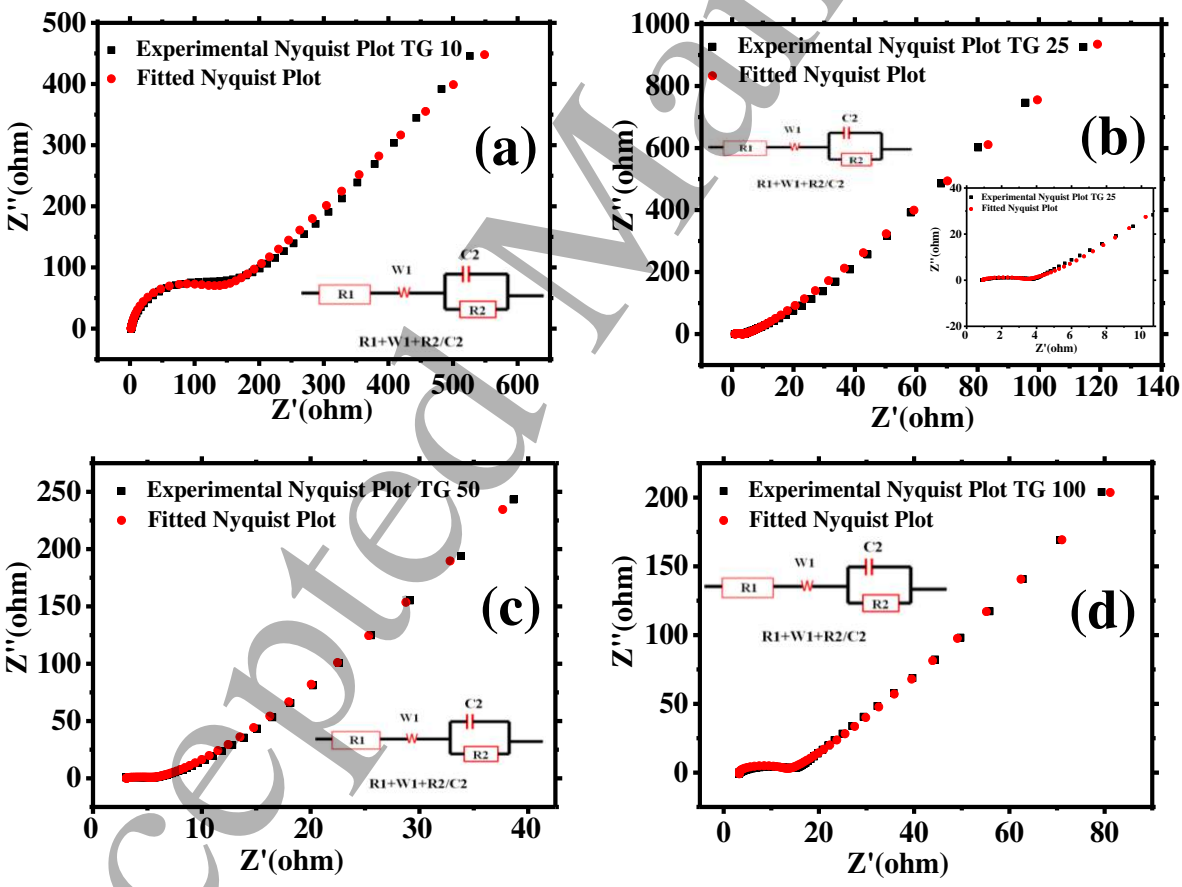

Figure 6: Typical Nyquist plots fitted with equivalent circuit diagram (inset) for different compositions based supercapacitor (a) TG 10, (b) TG 25, (c) TG 50 and (d) TG 100.

To investigate the origin of high specific capacitance, electrochemical impedance measurements were carried out over a frequency range from 0.001 Hz to 10 kHz. Figure 6 shows the Nyquist plots of the all compositions of GO-TiO_2 nanocomposite based supercapacitors. Nyquist plot for each composition shows a single semicircle and straight line slope in the high-frequency region and low frequency regions, respectively. The sloping straight line in the low frequency region is attributed to the ion diffusion/transportation in the electrode, and the single semicircle corresponds to the interfacial charge-transfer resistance between electrodes and electrolyte. Charge transfer resistance (R_{ct}) values of TG10, TG25, TG50, and TG100 based supercapacitors are calculated to be 113.5, 2.3, 3.1, 9.3 ohm, respectively after fitting the Nyquist plot in the equivalent circuit shown in the inset of Figure 6 a-d. It is found that R_{ct} value for TG25 based supercapacitor is the lowest and that's the reason for high specific capacitance value of TG25 based supercapacitors.[32] The equivalent series resistance (ESR) values are found to be 1.64, 0.82, 2.30 and 3.17 Ω, deduced from the point of the curve intersection with a lateral axis for TG10, TG25, TG50 and TG100, respectively. ESR is the sum of electrolyte resistance, intrinsic resistance of the active materials and the contact resistance between electrode electrolyte interfaces. The low value of ESR confirms a good contact between electrode materials and current collector (steel) and a small resistance between the electrode and electrolyte interfaces.

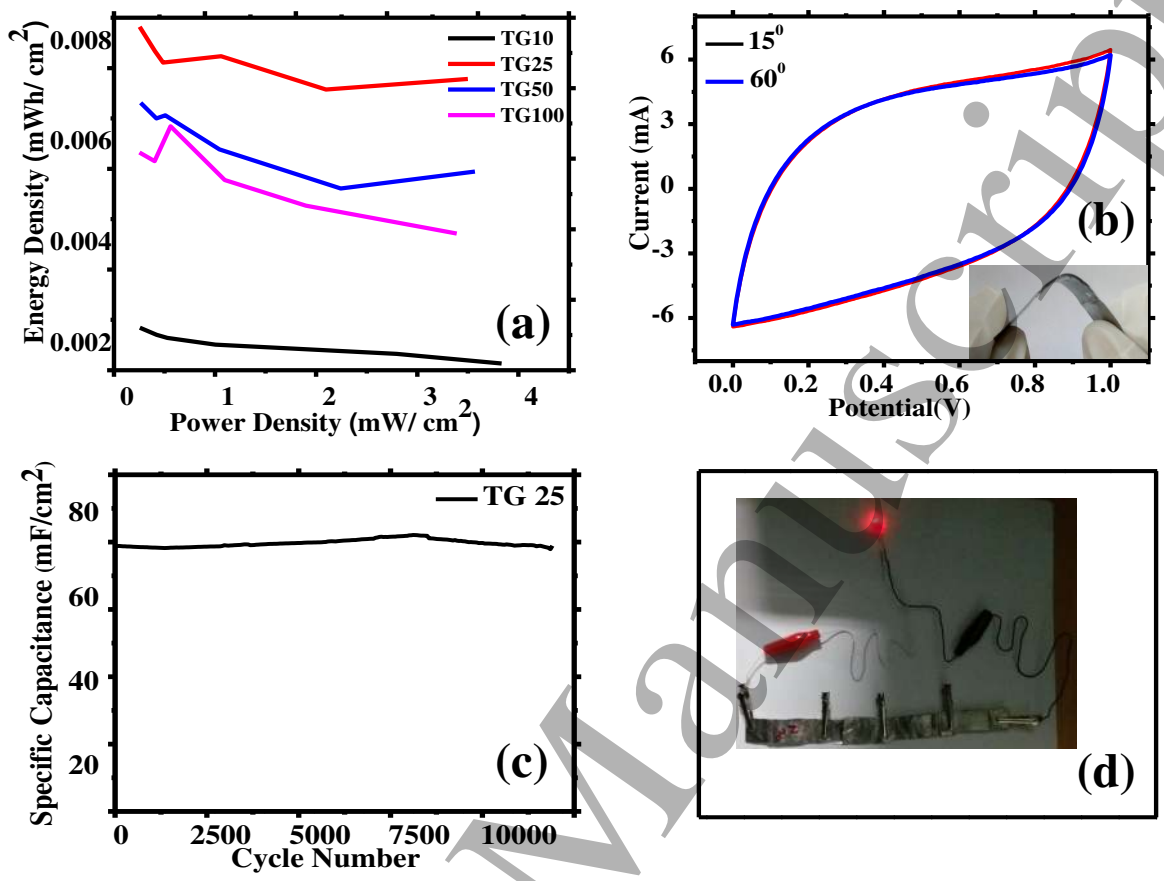

Figure 7: (a) Comparative Ragone plot of different compositions based device; (b) comparison of CV curves at different bending angles; (c) Cyclic stability of the TG25 based device; (d) LED illumination using fabricated supercapacitor.

Ragone plots shown in Figure 7(a) describe the corresponding relation between the specific energy density (E) and the specific power density (P), which are the main parameters that reflects the electrochemical performances of the supercapacitors. The energy densities of the TG25 supercapacitor were dramatically higher compared with that of other composites based supercapacitor, especially in cases with lower power densities (Table S3, ESI), indicating it as an ideal composition to get superior performances.

The flexibility of the devices is also tested by measuring the CV curve at different bending angles. The unaltered CV curves (Figure 7b) at different bending angles confirm the nanocomposites as a potential candidate for flexible energy storage technology. Interestingly, the TG25 based supercapacitor device shows high (92%) specific capacitance retention after continuous 10,000 charge discharge cycles (7 c). Finally, to provide a clear evidence of the electrical charge storage property, we have illuminated a red LED, as shown in Figure 7(d) and video S1 in the ESI. A series combination of three supercapacitors is charged by applying 2V for 3 min. After disconnecting it from the voltage sources, it glows the red LED for 5 min and then it starts discharging and fully discharged within next 5 min.

Conclusions:

In this article, mesoporous GO-TiO_2 nanocomposites consisting varying proportion of GO are synthesized by a simple, easy, fast and controlled HCl catalyzed method for flexible solid-state supercapacitor applications. Evolutions of TiO_2 nanospindles of rutile phase on graphene platform are monitored by SEM, TEM, XPS, XRD and Raman analysis. Employing, a new combination of GO-TiO_2 as electrode active layer material and PVA-H_3PO_4 as gel electrolyte, a high performance solid-state supercapacitor is realized. The GO-TiO_2 composites based flexible solid-state supercapacitor show a high specific capacitance of 73.43 mF/cm^2 at a current density of 0.5 mA /cm^2 and 92% retention of specific capacitance after 10,000 continuous charge-discharge cycles. The superior performance of TiO_2 nanospindles grafted GO based supercapacitor (TG25) is originated from its large surface area of mesoporous structure of TG25 and intimate contact between graphene oxide and TiO_2. Finally, three supercapacitors in a series

have illuminated a red LED, indicating the material as a potential candidate for energy storage technology.

Acknowledgments:

This work is supported by Department of Science and Technology, Govt. of India. (Grant No IFA 13-MS-09).The authors are greatly thankful to Prof. Madhab C Das of Department of chemistry for fruitful discussion on BET adsorption isotherm analysis.

[1] Brezesinski T, Wang J, Polleux J, Dunn B and Tolbert S H 2009 Templated nanocrystal-based porous TiO2 films for next-generation electrochemical capacitors *J. Am. Chem. Soc.* **131** 1802–9

[2] Ke Q, Liao Y, Yao S, Song L and Xiong X 2016 A three-dimensional TiO2/graphene porous composite with nano-carbon deposition for supercapacitor *J. Mater. Sci.* **51** 2008–16

[3] Salari M, Konstantinov K and Liu H K 2011 Enhancement of the capacitance in TiO2nanotubes through controlled introduction of oxygen vacancies *J. Mater. Chem.* **21** 5128–33

[4] Huang M, Li F, Dong F, Zhang Y X and Zhang L L 2015 MnO2-based nanostructures for high-performance supercapacitors *J. Mater. Chem. A* **3** 21380–423

[5] Rakhi R B, Chen W, Cha D and Alshareef H N 2011 High performance supercapacitors using metal oxide anchored graphene nanosheet electrodes *J. Mater. Chem.* **21** 16197–204

[6] Xie L J, Wu J F, Chen C M, Zhang C M, Wan L, Wang J L, Kong Q Q, Lv C X, Li K X

and Sun G H 2013 A novel asymmetric supercapacitor with an activated carbon cathode and a reduced graphene oxide-cobalt oxide nanocomposite anode *J. Power Sources* **242** 148–56

[7] Lang X, Hirata A, Fujita T and Chen M 2011 Nanoporous metal/oxide hybrid electrodes for electrochemical supercapacitors *Nat. Nanotechnol.* **6** 232–6

[8] Elmouwahidi A, Bailón-García E, Castelo-Quibén J, Pérez-Cadenas A F, Maldonado-Hódar F J and Carrasco-Marín F 2018 Carbon-TiO2 composites as high-performance supercapacitor electrodes: Synergistic effect between carbon and metal oxide phases *J. Mater. Chem. A* **6** 633–44

[9] Zhang Y, Zhao Y, Cao S, Yin Z, Cheng L and Wu L 2017 Design and Synthesis of Hierarchical SiO2@C/TiO2Hollow Spheres for High-Performance Supercapacitors *ACS Appl. Mater. Interfaces* **9** 29982–91

[10] W. Lai C, W. Low F, W. Chong S, P.P. Wong C, Binti Mohamed Siddick S Z, C. Juan J and B. Abdul Hamid S 2015 An Overview: Recent Development of Titanium Dioxide Loaded Graphene Nanocomposite Film for Solar Application *Curr. Org. Chem.* **19** 1882–95

[11] Ding Q, Li W L, Zhao W L, Wang J Y, Xing Y P, Li X, Xue T, Qi W, Zhang K L, Yang Z C and Zhao J S 2017 Plasma assisted fabrication of multi-layer graphene/nickel hybrid film as enhanced micro-supercapacitor electrodes *IOP Conf. Ser. Mater. Sci. Eng.* **182** 012014

[12] Yang Y C, Huang W Q, Xu L, Hu W, Peng P and Huang G F 2017 Hybrid

TiO2/graphene derivatives nanocomposites: Is functionalized graphene better than pristine graphene for enhanced photocatalytic activity? *Catal. Sci. Technol.* **7** 1423–32

[13] Zhang L, Zhang F, Yang X, Long G, Wu Y, Zhang T, Leng K, Huang Y, Ma Y, Yu A and Chen Y 2013 Porous 3D graphene-based bulk materials with exceptional high surface area and excellent conductivity for supercapacitors *Sci. Rep.* **3** 1408

[14] Ghosh S, Calizo I, Teweldebrhan D, Pokatilov E P, Nika D L, Balandin A A, Bao W, Miao F and Lau C N 2008 Extremely high thermal conductivity of graphene: Prospects for thermal management applications in nanoelectronic circuits *Appl. Phys. Lett.* **92** 151911

[15] Li Z F, Zhang H, Liu Q, Sun L, Stanciu L and Xie J 2013 Fabrication of high-surface-area graphene/polyaniline nanocomposites and their application in supercapacitors *ACS Appl. Mater. Interfaces* **5** 2685–91

[16] Peng G, Ellis J E, Xu G, Xu X and Star A 2016 In Situ Grown TiO2Nanospindles Facilitate the Formation of Holey Reduced Graphene Oxide by Photodegradation *ACS Appl. Mater. Interfaces* **8** 7403–10

[17] Han J T, Kim B J, Kim B G, Kim J S, Jeong B H, Jeong S Y, Jeong H J, Cho J H and Lee G W 2011 Enhanced electrical properties of reduced graphene oxide multilayer films by in-situ insertion of a TiO2layer *ACS Nano* **5** 8884–91

[18] Xiang C, Li M, Zhi M, Manivannan A and Wu N 2012 Reduced graphene oxide/titanium dioxide composites for supercapacitor electrodes: Shape and coupling effects *J. Mater. Chem.* **22** 19161–7

[19] Salari M, Aboutalebi S H, Chidembo A T, Nevirkovets I P, Konstantinov K and Liu H K 2012 Enhancement of the electrochemical capacitance of TiO 2 nanotube arrays through controlled phase transformation of anatase to rutile *Phys. Chem. Chem. Phys.* **14** 4770–9

[20] Kim J, Khoh W H, Wee B H and Hong J D 2015 Fabrication of flexible reduced graphene oxide-TiO2 freestanding films for supercapacitor application *RSC Adv.* **5** 9904–11

[21] Midya A, Mamidala V, Yang J X, Ang P K L, Chen Z K, Ji W and Loh K P 2010 Synthesis and superior optical-limiting properties of fluorene-thiophene- benzothiadazole polymer-functionalized graphene sheets *Small* **6** 2292–300

[22] Midya A, Mukherjee S, Roy S, Santra S, Manna N and Ray S K 2018 Selective chloroform sensor using thiol functionalized reduced graphene oxide at room temperature *Mater. Res. Express* **5** 025604

[23] Liang Y, Wang H, Casalongue H S, Chen Z and Dai H 2010 TiO2Nanocrystals grown on graphene as advanced photocatalytic hybrid materials *Nano Res.* **3** 701–5

[24] Sher Shah M S A, Park A R, Zhang K, Park J H and Yoo P J 2012 Green synthesis of biphasic TiO2-reduced graphene oxide nanocomposites with highly enhanced photocatalytic activity *ACS Appl. Mater. Interfaces* **4** 3893–901

[25] Lin J, Wang B, Sproul W D, Ou Y and Dahan I 2013 Anatase and rutile TiO2films deposited by arc-free deep oscillation magnetron sputtering *J. Phys. D. Appl. Phys.* **46** 084008

[26] Wu M, Long J, Huang A, Luo Y, Feng S and Xu R 1999 Microemulsion-mediated

hydrothermal synthesis and characterization of nanosize rutile and anatase particles *Langmuir* **15** 8822–5

[27] Moon G D, Joo J B, Dahl M, Jung H and Yin Y 2014 Nitridation and Layered Assembly of Hollow TiO 2 Shells for Electrochemical Energy Storage *Adv. Funct. Mater.* **24** 848–56

[28] Liu W W, Yan X Bin and Xue Q J 2013 Multilayer hybrid films consisting of alternating graphene and titanium dioxide for high-performance supercapacitors *J. Mater. Chem. C* **1** 1413–22

[29] Ramadoss A, Kim G S and Kim S J 2013 Fabrication of reduced graphene oxide/TiO2 nanorod/reduced graphene oxide hybrid nanostructures as electrode materials for supercapacitor applications *CrystEngComm* **15** 10222–9

[30] Lv Q, Chi K, Zhang Y, Xiao F, Xiao J, Wang S and Loh K P 2017 Ultrafast charge/discharge solid-state thin-film supercapacitors via regulating the microstructure of transition-metal-oxide *J. Mater. Chem. A* **5** 2759–67

[31] Zheng B, Huang T, Kou L, Zhao X, Gopalsamy K and Gao C 2014 Graphene fiber-based asymmetric micro-supercapacitors *J. Mater. Chem. A* **2** 9736–43

[32] Suroshe J S and Garje S S 2015 Capacitive behaviour of functionalized carbon nanotube/ZnO composites coated on a glassy carbon electrode *J. Mater. Chem. A* **3** 15650–60